



1 Nitrogen limitation information retrieved from data 2 assimilation

3 Song Wang^{1,2,3}, Carlos A. Sierra³, Yiqi Luo⁴, Jinsong Wang^{1,2}, Weinan Chen^{1,2}, Yahai
4 Zhang^{3,5}, Aizhong Ye⁵, Shuli Niu^{1,2}

5 ¹Key Laboratory of Ecosystem Network Observation and Modeling, Institute of Geographic Sciences
6 and Natural Research, Chinese Academy of Sciences, Beijing 100101, China.

7 ²College of Resources and Environment, University of Chinese Academy of Sciences, Beijing 100049,
8 China.

9 ³Department of Biogeochemical Processes, Max Planck Institute for Biogeochemistry, Jena, 07745,
10 Germany.

11 ⁴School of Integrative Plant Science, Cornell University, NY 14853, USA.

12 ⁵State Key Laboratory of Earth Surface Processes and Resource Ecology, Faculty of Geographical
13 Science, Beijing Normal University, Beijing 100875, China.

14 *Corresponding to:* Shuli Niu (sniu@igsnr.ac.cn)

15 **Abstract:** Nitrogen (N) limitation greatly constrains terrestrial ecosystem carbon (C) uptake and its
16 response to climate change and elevated carbon dioxide. Hence, accurate assessments of ecosystem N
17 limitation are crucial for predicting C-N feedbacks, and vital for providing guidance for policy making
18 or ecosystem management as well. This study aims to retrieve N limitation information by data model
19 fusion from one field N addition experiment so that we can better understand N controls on the terrestrial
20 C cycle. We estimated two sets of parameters with one C-only model and one coupled C-N model. Our
21 results showed that the estimated leaf photosynthetic efficiency (LPE) and process rates (e.g., senescence
22 and decomposition rates) of organic C from almost all pools were higher with the coupled C-N model
23 than those with the C-only model at the ambient treatment. However, the differences in the LPE and the
24 C exit rates between the coupled C-N model and the C-only model decreased with the increasing N
25 addition rates. Both the C-only and coupled C-N models simulated similar C pool sizes as observed at
26 every N addition treatment with their respective parameter estimates. However, simulated ecosystem C
27 storage and gross primary productivity (GPP) decreased if we ran the coupled C-N model with the
28 parameters estimated by the C-only model. This decrease was larger at the ambient treatment and became
29 smaller with the increase of N addition. In general, we put forward a new method to retrieve N limitation
30 information from observations by data model fusion. This method will make it possible to estimate the



31 global nutrient limitation and benefit ecosystem management and policy making.

32 **Keywords:** Data assimilation, nitrogen limitation information, nitrogen addition, model structure,
33 carbon and nitrogen cycles.

34 1. Introduction

35 Nitrogen (N) availability is a key limiting factor for growth in many terrestrial ecosystems, and thus
36 important for both ecosystem productivity and the decay of dead organic material (Keeler et al., 2009;
37 Liu et al., 2019; Pregitzer et al., 2010). As a consequence, plant tissue N content is often highly correlated
38 with key metabolic rates such as photosynthesis (Zong et al., 2018) and respiration (Sun et al., 2014),
39 and an important control on the turnover of soil organic matter (Fog, 2008; Keeler et al., 2009).
40 Manipulative N addition experiments and field studies have demonstrated larger plant growth with
41 increasing N deposition (LeBauer and Treseder, 2008; Pregitzer et al., 2010). Hence, the capacity of
42 terrestrial ecosystems to store carbon (C) is limited by its N availability and the C:N stoichiometry of
43 plant tissue (Hungate et al., 2003; Luo et al., 2004), especially under elevated atmospheric CO₂
44 concentrations.

45 An accurate assessment of ecosystem N limitation is crucial for predicting C cycle and its feedback
46 to climate change, which remain one of the biggest uncertainties in earth system models (Friedlingstein
47 et al., 2022). One important source of uncertainty in predicting C cycle is the degree to which N limits
48 plant growth (Elser et al., 2007; Hungate et al., 2003). Furthermore, the N limitations in plant growth,
49 photosynthetic capacity, and decomposition rates in litter and soil are poorly understood partially because
50 they are very difficult to be measured (Vicca et al., 2018). Some methods have been used to infer nutrient
51 limitation, including fertilization experiments, leaf nutrient resorption efficiency and the thresholds of
52 leaf N:P ratios (Bracken et al., 2015; Du et al., 2020; Sullivan et al., 2014; Tessier and Raynal, 2003).
53 But most of these methods are either very time-consuming and laborious, or have greater uncertainty,
54 although researchers have invested a lot of efforts to use these methods to retrieve nitrogen limitation
55 information in terrestrial ecosystems.

56 Data assimilation is a statistically rigorous method for estimating the parameter values of a mechanistic
57 model representing rates of transfer of C and N within an ecosystem. Not only does this method allow
58 models to be better calibrated to data, but it also provides great opportunities to understand model
59 parameterization that reflects N-limitation. When data assimilation is applied to calibrate models with



60 specific observations, the information in observations is integrated into the model via a set of specific
61 parameters (Luo and Schuur, 2020). All data assimilation studies indicate that the optimal estimated
62 parameters vary across different treatments of global change experiments (Liang et al., 2018; Luo and
63 Schuur, 2020; Wang et al., 2021; Xu et al., 2006). Because there are always some processes at unresolved
64 scales (processes that can't be represented explicitly) that may potentially interact with processes at
65 resolved scales (processes that can be represented explicitly) to influence model results. Varying
66 parameters is a useful modeling approach, which recognizes that the model need not explicitly
67 incorporate all processes on a resolved scale (Luo and Schuur, 2020). Meanwhile, the estimated
68 parameters are the result of retrieving the ecological information from the specific data set. Hence, many
69 studies used data assimilation to understand ecological processes (e.g., coefficients of plant allocation
70 and litter decomposition) by comparing the posterior probability density functions of parameter values
71 among different experimental treatments or sites (Liang et al., 2018; Wang et al., 2021; Xu et al., 2006).

72 Therefore, data assimilation provides the great possibility to retrieve N limitation information from
73 observations since the N limitation information is represented in parameterization as a model is calibrated
74 with the observations (Luo and Schuur, 2020). However, when a N cycle module is incorporated into the
75 C-only model, N processes are explicitly represented and simulated. N limitation influences on C
76 processes are no longer accounted by C-related parameter values (Wang et al., 2022). A study using data
77 assimilation technique found that parameter values change with model structures, while simulated
78 ecosystem C dynamics were similar (Wang et al., 2022), but they didn't further explore the nutrient
79 limitation information behind models with different structures and how it influenced the C cycle
80 predictions. Previous studies also tried to use models with or without a nutrient module to represent
81 whether there was the corresponding nutrient limitation (i.e., nitrogen and phosphorus) with data
82 assimilation (Du et al., 2021). But they ignored the fact that the nutrient limitation information in the C-
83 only model and C-nutrient coupling model is consistent because the observations they used for data
84 assimilation were identical. Hence, it's necessary to retrieve information on nutrient limitation by data
85 assimilation.

86 In this study, we used data assimilation to estimate parameters that reflect N limitation in a C-only
87 model and coupled C-N model from 17 data sets collected at a field N enrichment experiment at an alpine
88 meadow in the Qinghai-Tibet Plateau. The Bayesian probabilistic inversion as the data assimilation



89 method was used in this study to estimate the C cycle associated parameters and simulated C pool
90 dynamics of different ecosystem components under the integral measurement collected at Hong Yuan
91 alpine meadow field site from 2014 to 2020. The specific questions we addressed in this study are: (1)
92 how to retrieve N limitation information from experimental data by data assimilation? (2) how does N
93 limitation influence the predictions of ecosystem C dynamic?

94 **2. Materials and methods**

95 **2.1 Site description**

96 The Hong Yuan station was located on the eastern Qinghai-Tibet Plateau (32°84'N, 102°58'E), which is
97 high elevation continental plateau with a frigid temperate monsoon climate. The mean annual
98 precipitation is 747 mm, the mean annual temperature is 1.5°C, the sunshine duration per year is about
99 2000-2400 hours, and the growing season lasts from April to October. The main vegetation type in this
100 study area is alpine meadow, and the soil type here is subalpine meadow and boggy soil (Song et al.,
101 2014). This area is dominated by *Deschampsia caespitosa* (Linn.) Beauv., *Koeleria cristata* (Linn.) Pers.,
102 *Gentiana sino-ornata* Balf. f., *Potentilla anserina* L., and *Anemone rivularis* Buch.-Ham (Quan et al.,
103 2018).

104 **2.2 Data source**

105 Data sets used to drive the Grassland ECOSystem (GECO) model and used to estimate parameters in
106 this study both were from a N addition experiment and a co-located eddy-covariance measurement
107 system. Meteorological variables, such as soil volumetric water content (VWC) and soil temperature
108 (Tsoil) simultaneously measured with the eddy covariance system at a depth of 10 cm every hour.
109 Meanwhile, the photosynthetically active radiation, wind speed, relative humidity, and air temperature
110 used for simulating photosynthesis also come from the continuous observation of the eddy covariance
111 system. The N addition experiment near the Eddy covariance tower used a random block design with six
112 N addition treatments (N0, N2, N4, N8, N16, N32, representing N addition rates of 0, 2, 4, 8, 16, 32 g
113 N·m⁻²·year⁻¹, respectively, with five replications each). The area of each plot is 8 × 8 m, and the distance
114 between adjacent quadrats is 3 m. During the growing season, from May to September every year, N was
115 added once a month. The method of N addition was spraying, and ammonium nitrate (NH₄NO₃, analytical
116 purity, content ≥ 99%) was used as N fertilizer. Gross primary productivity (GPP) and soil respiration



117 (SR) were measured twice a month with static chambers (LI-6400XT, LI-COR Environmental, Lincoln,
118 Nebraska, USA) in plots with different treatments in the growing season from 2014 to 2020. Biometric
119 measurements were made once a year to determine leaf and root biomass, standing and surface litter
120 quality, and microbes, soil C content, N content of leaves and roots, standing litter, surface litter, total N
121 content of microbe and soil, and soil inorganic N concentration in all plots.

122 The data that used to drive the model includes daily soil moisture, soil temperature, photosynthetically
123 active radiation, wind speed, relative humidity, and air temperature from 2014 to 2020. The data
124 assimilated into the GECO model for parameter estimation include C and N contents in leaf, root,
125 standing litter, surface litter, microbial, soil, and autotrophic and heterotrophic respiration at every N
126 addition treatment (Table S1).

127 **2.3 Model**

128 The GECO model was used in this study (Wang et al., 2021), which has evolved from the Terrestrial
129 ECOsystem (TECO) model (Xu et al. 2006, Shi et al. 2016) with a distinct standing litter pool for
130 grassland ecosystems. The GECO model has both coupled C-N and C-only version. There are seven C
131 and N pools and one more mineral nitrogen pool in the coupled C-N model. The pools are leaf (X1, N1),
132 roots (X2, N2), standing litter (X3, N3), surface litter (X4, N4), fast (X5, N5), slow (X6, N6), passive
133 soil organic matter (SOM, X7, N7) and mineral N pool (Fig. 1). But the C-only model just has the
134 counterpart C pools. In the GECO model, CO₂ in the atmosphere enters the ecosystem by canopy
135 photosynthesis which is simulated by a two-leaf model (Wang et al., 1998). The plant photosynthetic
136 capacity is limited by the leaf N concentration in the coupled C-N model, reflecting plant investment in
137 photosynthetic machinery for light harvesting and carboxylation rates (Leuning et al., 1995; Walker et
138 al., 2015). Leaf photosynthetic efficiency (LPE) limited by foliage N content as a scalar:

$$139 \quad SNvcmax = \max \left(\min \left(\exp \left(- \frac{CN_{leaf} - CN_{leaf,0}}{CN_{leaf,0}} \right), 1 \right), 0 \right) \quad (1)$$

140 where CN_{leaf} is the estimated C:N ratio of foliage and $CN_{leaf,0}$ is the defined C:N ratio of foliage without
141 N limitation. Some of the photosynthates were used for plants' respiration, and the remaining assimilated
142 C was allocated to leaf (X1) and root (X2) pools. Detritus from the dead plants then flowed into the litter
143 pool, which contained standing litter (X3) and surface litter (X4). Some of the subsurface litter was
144 respired by microbes, while the rest was converted to fast SOM (X5) and slow SOM (X6). The CO₂

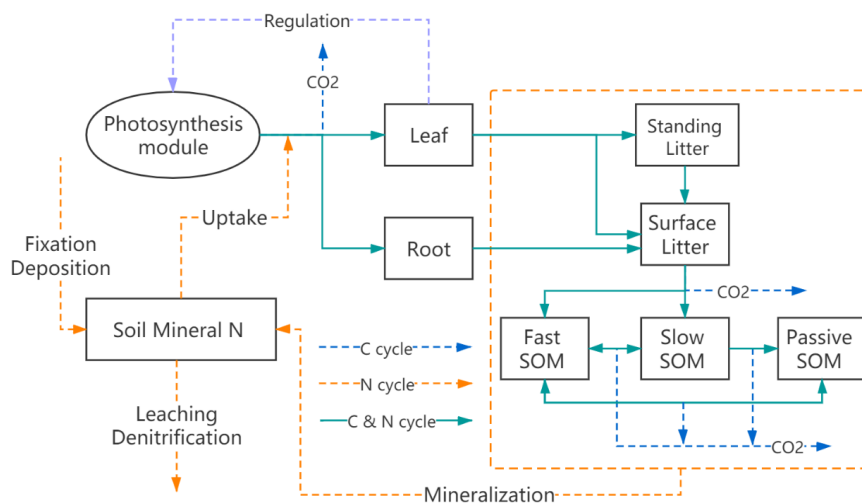


145 released by the decomposition of soil C eventually re-enters the atmosphere. Similarly, plants uptake N
 146 from the mineral soil. Subsequently, the uptaken N is distributed to the plant pools and then transferred
 147 to the litter and soil pools. The organic N in the seven pools returns to the soil through microbial
 148 mineralization. The GECO model uses a matrix-based 1st-order differential equation approach to
 149 describe the process of carbon transfer between ecosystem carbon pools as:

$$\frac{d}{dt} \mathbf{X}(t) = \mathbf{A} \xi(t) \mathbf{K} \mathbf{N}_s \mathbf{X}(t) + \mathbf{b} u(t) \quad (2)$$

$$\mathbf{X}(0) = \mathbf{X}_0$$

152 where $\mathbf{X} = (x_1 \ x_2 \ x_3 \ x_4 \ x_5 \ x_6 \ x_7)^T$, in which $x_{(i)}$ represents the C pools in leaves, roots, standing litter,
 153 surface litter, fast, slow and passive SOM at time t . The matrix \mathbf{A} represents C transfer between pools
 154 (Xu et al., 2006). \mathbf{K} is a 7×7 diagonal matrix with diagonal entries. The elements on the diagonal indicate
 155 the C processing rates of each pool ($i = 1, 2, \dots, 7$). \mathbf{N}_s is a 7×7 diagonal matrix with diagonal entries,
 156 elements on the diagonal indicate the N limiting effects on the pools decomposition rates, which is
 157 represented by $N_s(i) = \exp((CN_0 - CN(i))/CN_0)$ ($i = 1, 2, \dots, 7$). For the C-only model, there is no any
 158 diagonal matrix to represent the N limitation effects. u represents the C produced by canopy
 159 photosynthesis, which is constrained by equation (1). \mathbf{b} is a vector of partitioning coefficients of
 160 photosynthetic products to leaves and roots. $\xi(t)$ is an environmental scalar to account for effects of
 161 temperature and humidity on decomposition (Luo et al., 2003).



162
 163 **Figure 1 Carbon and nitrogen pools and flux pathways in GECO model. Blue arrows show carbon transfer**
 164 **processes, yellow arrows indicate nitrogen transfer processes, and green arrows represent C and N coupling**



165 **processes. SOM, soil organic matter.**

166 In the coupled C-N model, the N processes can be described by this formula:

$$167 \quad \frac{d}{dt} \mathbf{N}(t) = \mathbf{A}\xi(t) \mathbf{K} \mathbf{N}_s \mathbf{R}^{-1} \mathbf{X}(t) + \kappa_\mu N_{min}(t) \boldsymbol{\pi} \quad (3)$$

$$168 \quad \mathbf{N}(0) = \mathbf{N}_0$$

169 where $\mathbf{N} = (n_1 \ n_2 \ n_3 \ n_4 \ n_5 \ n_6 \ n_7)^T$, in which $n_{(i)}$ represents the N pools in leaves, roots, standing litter,
170 surface litter, fast, slow and passive SOM at time t . \mathbf{R} is a 7×7 diagonal matrix with diagonal elements
171 indicating the C:N ratio of each pool. $\boldsymbol{\pi} = (\pi_1 \ 1 - \pi_1 \ 0 \ 0 \ 0 \ 0 \ 0)^T$ is an allocation coefficient vector of N from
172 mineral soil to leaves and roots. κ_μ is N uptake rate of plants, $N_{min}(t)$ is the amount of available N in
173 the soil at time t . The dynamic equilibrium of mineral N in soil is determined by the input of
174 mineralization, biological fixation, atmospheric deposition, the output of plant input, leaching, and
175 gaseous N fluxes, which can be described by:

$$176 \quad \frac{d}{dt} N_{min}(t) = -(\kappa_u + \kappa_L) N_{min}(t) + \mathbf{A}\xi(t) \boldsymbol{\varphi}_1^* \mathbf{K} \mathbf{N}_s \mathbf{R}^{-1} \mathbf{X}(t) + F(t) \quad (4)$$

$$177 \quad N_{min}(0) = N_{min,0}$$

178 In formula (4), κ_u and κ_L represent rates of N uptake and N loss, respectively. $\mathbf{A}\xi(t) \boldsymbol{\varphi}_1^* \mathbf{K} \mathbf{N}_s \mathbf{R}^{-1} \mathbf{X}(t)$
179 represents N mineralization, $\boldsymbol{\varphi}_1^*$ represents mineralization rate, and $F(t)$ represents N input by biological
180 fixation and atmospheric deposition.

181 In this study, the initial pool sizes of leaves, roots, standing litter, surface litter, fast soil, slow soil, and
182 passive soil pools were constrained using ambient treatment data. The same values used in the ambient
183 treatment were used for initial pool sizes in the N addition treatment, assuming that there was no
184 significant difference between the ambient and supplemental N treatments before treatment began.

185 Compared with the coupled C-N model, the C-only model doesn't contain any N-cycle process. In
186 this study, the C exit rates of 7 pools, the C allocation coefficients of GPP, and the C transfer coefficients
187 were estimated using both the C-only model and the coupled C-N model. Meanwhile, N-related
188 parameters such as N partitioning coefficient, N uptake, N loss, external N input, initial mineral N pool,
189 and C:N ratios of different ecosystem components were estimated in the coupled C-N model.

190 **2.4 Data assimilation**

191 We used Markov-Chain Monte-Carlo (MCMC) to estimate parameters values of the GECCO model. In
192 this method, the targeted parameters are considered as random variables within to a certain prior
193 probability distribution. According to the Bayesian theorem, the prior knowledge about the parameters



194 and the information contained in the data are fused to generate posterior distributions of the parameters
195 (Xu et al., 2006) as

$$196 \quad P(p|Z) \propto P(Z|p)P(p) \quad (5)$$

197 In formula 5, $P(p)$ and $P(p|Z)$ represent the prior probability density function (PDF) and posterior
198 probability density function (PPDF) of parameters, respectively. $P(Z|p)$ represents conditional
199 probability density of observation under the prior parameters, which is also called the likelihood function
200 of p . We assume that the random error is normally distributed and has a mean of zero, so the likelihood
201 function can be represented as follows:

$$202 \quad P(Z|p) \propto \exp \left\{ - \sum_{i=1}^{17} \sum_{t \in Z_i} \frac{[Z_i(t) - \varphi_i X(t)]^2}{2\sigma_i^2(t)} \right\} \quad (6)$$

203 In formula 6, $Z_i(t)$ and $\varphi_i X(t)$ represent the measured value and simulated values of the observed
204 variable i at time t , and σ_i is the standard deviation of the observed variable i . In this study, i from 1 to
205 17 represents seventeen data sets, which are the C or N contents of leaves, roots, standing litter, surface
206 litter, microbes, mineral soil and heterotrophic respiration, inorganic N in soil, soil mineralization, N
207 uptake by plant and external N input. φ_i is the mapping vector that maps the simulated state variables to
208 the observed data. For example, the observation operator φ is expressed as follows:

209 Leaf C and N: $\varphi_1 = (1 \ 0 \ 0 \ 0 \ 0 \ 0)$

210 Root C and N: $\varphi_2 = (0 \ 1 \ 0 \ 0 \ 0 \ 0)$

211 Standing litter C and N: $\varphi_3 = (0 \ 0 \ 1 \ 0 \ 0 \ 0)$

212 Surface litter C and N: $\varphi_4 = (0 \ 0 \ 0 \ 0.5 \ 0 \ 0)$

213 Microbial C and N: $\varphi_5 = (0 \ 0 \ 0 \ 0 \ 1 \ 0)$

214 Mineral soil C and N: $\varphi_6 = (0 \ 0 \ 0 \ 0 \ 1 \ 1)$

215 The Metropolis-Hastings (M-H) algorithm was used as the (Hastings, 1970; Metropolis et al., 1953)
216 MCMC sampler. The initial parameter set was randomly selected within the priori parameter ranges. At
217 each iteration, a set of parameters (p_{new}) is proposed based on the accepted parameters from the previous
218 iteration (p_{k-1}). We accept p_{new} only if $R = \frac{P(p_{\text{new}}|Z)}{P(p_{k-1}|Z)} \Rightarrow$ a random number between 0 and 1.

219 Otherwise, p_{new} will be rejected, and we let $p_k = p_{k-1}$ to start the sampling of next iteration. The M-H
220 algorithm is repeated until 300,000 sets of parameter values have been accepted, and then all accepted
221 parameter values are used to construct the probability distribution functions (PDFs) (Weng and Luo,
222 2011; Xu et al., 2006).

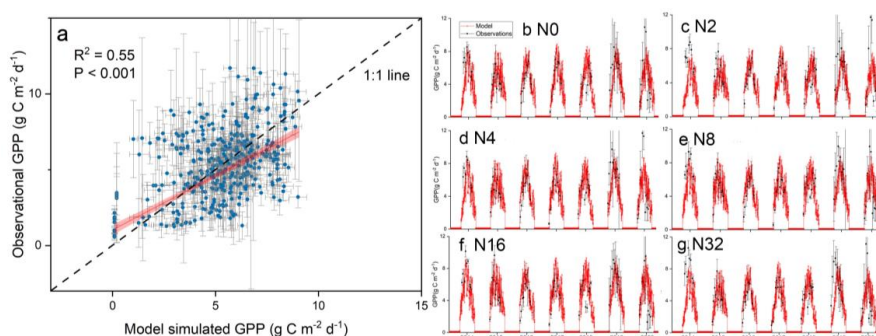
223 3. Results



224 3.1 Model performance on simulating C cycle under different N addition gradients

225 We selected 100 sets of parameter values from the PPDFs to run the GECO model and simulate the C
226 dynamics from 2014 to 2020 using the C-only model and the coupled C-N model, respectively. The two
227 models simulated the C pools in leaves, standing litter, surface litter, microbes, soil, and GPP well
228 compared to observations under the different N addition treatments (Figure 2 and Figure S1-S2).

229 Meanwhile, among 19 C-related parameters in both the C-only and coupled C-N models, nine were
230 well constrained by observations according to their posterior PDFs. These nine well-constrained
231 parameters are baseline leaf maximum carboxylation rate, C exit rates of root, leaf, standing litter, surface
232 litter, fast SOM, slow SOM, the allocation coefficients of C to root and leaf under all treatments. While
233 the C exit rate of the passive SOM and the transfer coefficients among pools ($f_{i,j}$) were poorly constrained.
234 In this study, we used the comparison of well estimated parameters between two models to indicate the
235 N limitation in the C cycle processes represented by these parameters, and used the comparison of
236 different C pool sizes between different models to indicate N limitation in the C pools as well.



237
238 **Figure 2** Comparison of observed and model-simulated GPP simulated by the coupled C-N model. **A** is the
239 overall comparison under different addition rate; **b, c, d, e, f, g** are the time dynamics of observed (dots) and
240 model-simulated (red lines) GPP simulated by the coupled C-N model under N0, N2, N4, N8, N16, N32
241 addition rate, respectively.

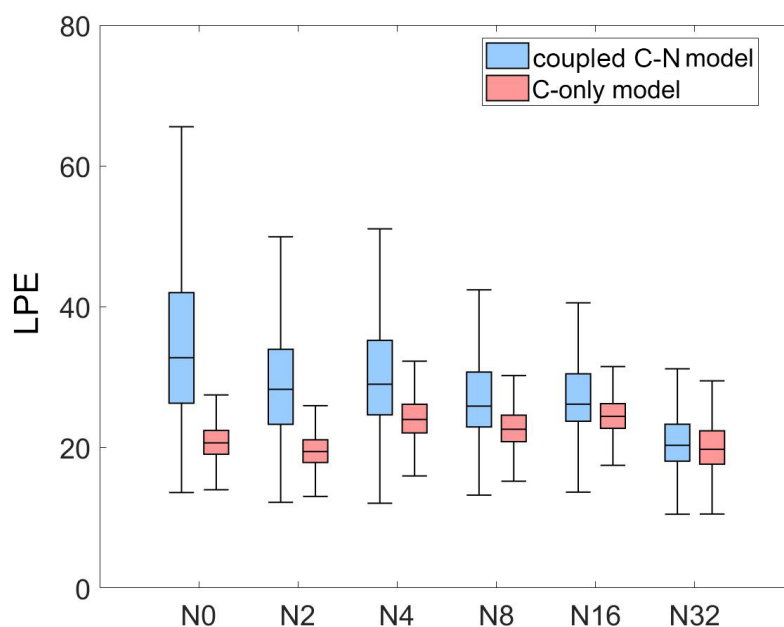
242 3.2 Estimated parameters between model structures and N addition treatments

243 The C-only and coupled C-N models led to different posterior PDFs of these well-constrained parameters
244 under the different treatments (Figures 3 and 4). The leaf photosynthetic efficiency (LPE) was higher in
245 the coupled C-N model than in the C-only model. But changes in estimated parameters between the C-
246 only and coupled C-N models differed with different N addition treatments. The estimated LPE
247 decreased with increasing N addition in the coupled C-N model, but the estimated LPE increased first

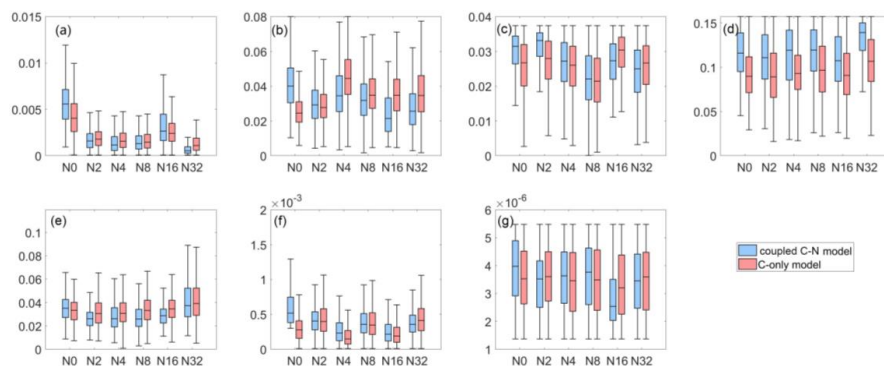


248 and then decreased with the increase of N addition in the C-only model. The divergent responses to N
249 addition treatments led to the results that the differences in the LPE between the coupled C-N model and
250 the C-only model got smaller with the increase of N addition rates (Figure 3).

251 C exit rates of all the pools were higher in the coupled C-N model than in the C-only model at the
252 ambient treatment (Figure 4). And with the increase of N addition rate (from N0 to N8), the differences
253 in the C exit rates of all the pools except the surface litter and fast SOM pools between the coupled C-N
254 model and the C-only model got smaller. But with the continuous increase of nitrogen addition (N16 &
255 N32), the differences of parameters between the C-only model and the coupled C-N model no longer
256 decreased, or even became greater. In general, the N addition effects on these parameters were consistent
257 in the C-only and coupled C-N model. N addition effects on parameterization varied among parameters.
258 C exit rate of the root pool decreased with the N addition rates, whereas the C exit rates of the standing
259 litter, fast SOM and slow SOM pools decreased first and then increased with the N addition rates. For
260 the remaining parameters, N addition didn't significantly change them (Figure 4).



261
262 **Figure 3** Posterior distributions of estimated leaf photosynthetic efficiency (LPE) of the C-only and coupled
263 C-N models under N0, N2, N4, N8, N16, N32 addition rate, respectively.



264
265 **Figure 4** Posterior distributions of estimated key parameters of the C-only and coupled C-N models under
266 different N addition treatments. Baseline senescence rates of fine root (a) and leaf (b); baseline decomposition
267 rates of standing litter (c), surface litter (d), fast SOM (e), slow SOM (f), and passive SOM (g). The red and
268 blue boxes represent the distributions of estimated parameters of the C-only and coupled C-N models,
269 respectively.

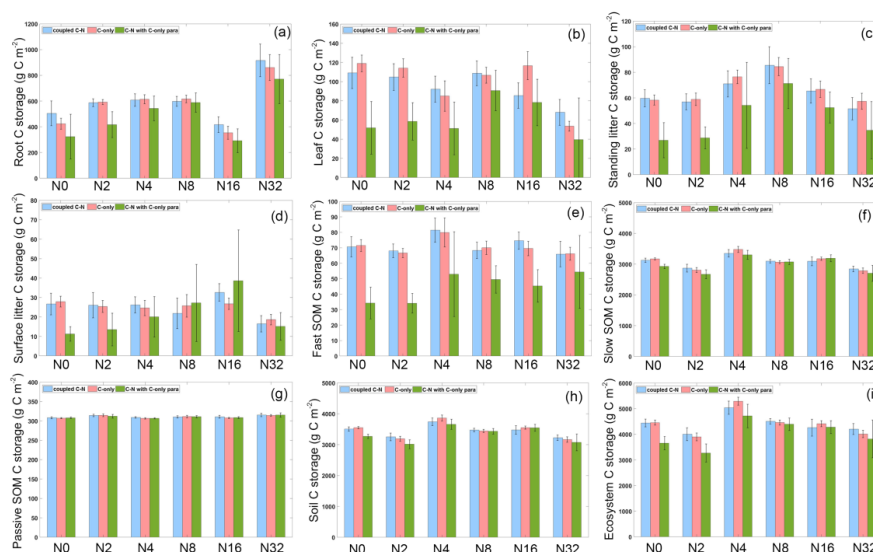
270 3.3 Simulations of C dynamics with the C-only and coupled C-N models

271 The different ecosystem C pools exhibited divergent responses to N addition treatments in the simulations
272 by both the C-only and coupled C-N models. Simulated passive SOM pools showed no N addition effects
273 (Figure 5g). Except for passive SOM pool, most of the rest carbon pool size increased first and then
274 decreased with the increase of N addition (Figure 5). Simulated leaf and surface litter C pools reached
275 the maximum pool size at N16 treatment (Figures 5a, 5d). Simulated standing litter reached the maximum
276 pool size at N8 treatment (Figure 5c). However, simulated fast and slow SOM C pools reached the
277 maximum pool size at N4 treatment (Figures 5e, 5f). Because the slow SOM C accounts for about 90%
278 of the total soil C and accounts for about 70% of the total ecosystem C, total soil C and ecosystem pools
279 responded similarly with slow SOM under the N addition treatments (Figure 5h, 5i). Meanwhile,
280 simulated GPP also showed a unimodal response with the increase of N addition and the maximum GPP
281 values appeared at N16 treatment in both the C-only and coupled C-N model (Figure 6).

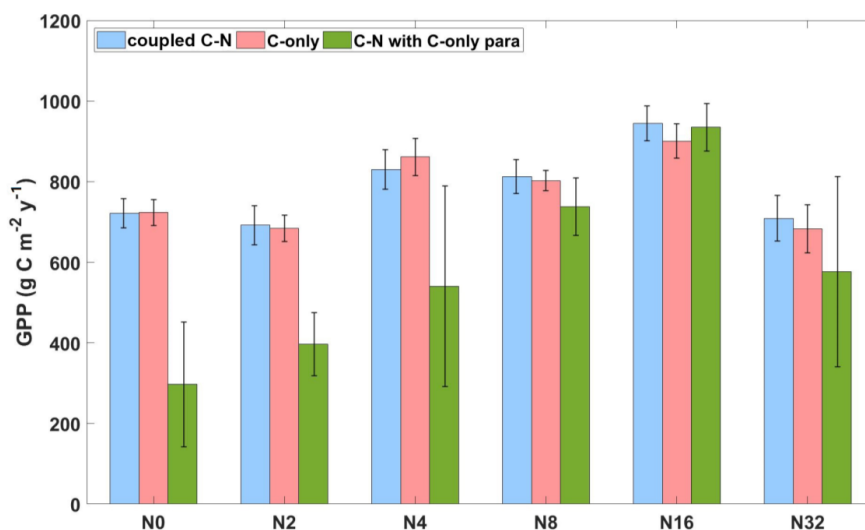
282 To further elucidate the N effects in the C only model, we tested the response of the coupled C-N
283 model without retuning parameters to compare the N limitation of ecosystem carbon pools and flux due
284 to the addition of N coupling components. The results showed that the simulated ecosystem C storage
285 and GPP decreased if we ran the coupled C-N model with the parameters estimated by the C-only model
286 (Figures 5 and 6). In addition, the decreased simulations by the coupled C-N model with the parameters
287 estimated by the C-only model were greater at the ambient treatment, and the decreases were reduced



288 with the increase of N addition (Figures 5 and 6). However, when the N addition reached at the N8
289 treatment, the difference between simulations by the coupled C-N model with the parameters estimated
290 by the C-only model and simulations by the coupled C-N model with its count part parameters became
291 very small. Hence, the simulations of the C-only, coupled C-N models and the coupled C-N model with
292 the parameters estimated by the C-only model were consistent at high N addition treatments
293 (Figures 5 and 6).



294
295 **Figure 5** Model simulated ecosystem C storage under different N addition treatments in 2020. They are root
296 (a), leaf (b), standing litter (c), surface litter (d), fast SOM (e), slow SOM (f), passive SOM (g), total soil C
297 storage (g) and total ecosystem (i) simulated by the C-only model with the C only parameters (blue bars), the
298 coupled C-N model with the coupled C-N parameters (red bars) and the coupled C-N model with the C only
299 parameters (green bars) under different N addition rates



300
301 **Figure 6** Model simulated GPP under different N addition treatments in 2020. Blue bar is ecosystem C storage
302 simulated by the C-only model with C-only parameters; Red bar is ecosystem C storage dynamic simulated
303 by the coupled C-N model with coupled C-N parameters; Green bar is ecosystem C storage dynamic simulated
304 by the coupled C-N model with C-only parameters.

305 4. Discussion

306 4.1 Retrieving N limitation information by data assimilation and its implications

307 In this study, we used data assimilation to retrieve N limitation information from observations. Our results
308 indicated that N limitation information can be retrieved by the following ways. First, the differences
309 between the parameters estimated by the C-only model and the coupled C-N model with the same
310 observation set. The parameters estimated by models with the data assimilation technique can represent
311 the C cycle processes of an ecosystem, e.g., GPP allocation to leaf and root are represented by two
312 allocation coefficients, and soil decomposition is represented by the soil exit rate. Because in the C-only
313 model, the N-related information contained in the observation is implicitly represented in the estimated
314 parameters. But when a coupled C-N model is calibrated using the same observations, the N-related
315 information is no longer implicitly represented in the C-related parameters (Wang et al., 2022). Second,
316 the differences between the C pool dynamic simulated by the coupled C-N model with parameters from
317 C-only model and the C pool dynamic simulated by the coupled C-N model with its counterpart
318 parameters (Figure 7), because the N limitation information behind parameters estimated by the C-only
319 model can be intuitively expressed by the simulations of ecosystem C pools. And our method in

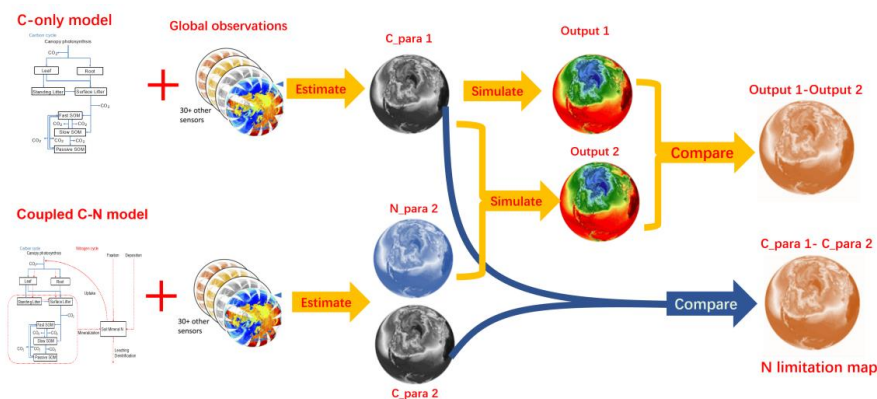


320 quantifying N limitation degree was confirmed by the N addition gradient in this study.

321 We highlight two main advantages of our method to retrieve nutrient limitation. On the one hand, by
 322 comparing the parameters shift and pools size, we can evaluate the N limitation effect on any specific C
 323 cycle processes of an ecosystem. And the N limitation degree can be quantitatively reflected by the
 324 differences between estimated parameters or simulated pool size. On the other hand, the data set used for
 325 data assimilation is no longer limited to nitrogen addition experiments. All of the observations which
 326 contain the basic C and N condition can be used to evaluate the N limitation by a C-only model and the
 327 coupled C-N model with data assimilation technique. In addition, there have been studies doing inverse
 328 analysis using global data products (Bloom et al., 2016; Yang et al., 2021), it will become possible to
 329 estimate the global nutrient limitation distribution by our method with increasing global data products
 330 with high reliability.

331 Due to the important effect of N on ecosystem C dynamics, it is vital to evaluate N limitation degree
 332 of an ecosystem. Understanding the N limitation condition at different areas can provide guidance for
 333 policy making and ecosystem management. Different managements should be conducted according to
 334 their N restriction condition of a specific ecosystem, so as to manage an ecosystem most efficiently.
 335 Besides, the N limitation in different C cycle processes and pools were poorly understood because it is
 336 hard to measure (Vicca et al., 2018). Our method can retrieve N limitation information of any specific
 337 ecosystem C cycle processes or pools, by which we can adjust ecosystem functions and services more
 338 accurately by precise management.

339



340

341 **Figure 7. A concept figure about how to map the global N limitation of a specific C pool.**

342 **4.2 Retrieve nitrogen limitation information from different C cycle processes**



343 In this study, we used two models: The C-only and coupled C-N models, to retrieve information on N
344 limitation. Our results show that the senescence rate from leaf and root, the decomposition rates of
345 standing litter, surface litter, fast SOM, slow SOM and passive SOM, the allocation coefficients of GPP
346 to leaf, and the LPE were higher in the C-N model than these in the C-only model at the ambient treatment
347 and lower in the N addition treatments (Figures 3, 4 and Figure S3). The N limitation degree was the
348 strongest at the ambient treatment, but the N regulations of C cycle processes are not explicitly simulated
349 and, thus, considered to be unresolved processes in the C-only model (Wang et al., 2022). Hence, the N
350 limitation on photosynthesis was reflected in a smaller value of LPE in the C-only model than that in the
351 coupled C-N model which incorporated a N module into the C model. Because N processes were
352 explicitly simulated in the coupled C-N model, N limitation effects on C processes were no longer
353 accounted by C-related parameter values (Figure 3). Meanwhile, the N limitation degree at the high N
354 addition treatments was much less than that at the ambient treatment (Figure S4). Therefore, differences
355 in the LPE between the coupled C-N model and the C-only model got smaller with the increase of N
356 addition rates (Figure 3), indicating that N limitation degree was reduced or even disappeared with the
357 increase of N addition rates. It needed to be specifically pointed out that we didn't consider any toxic
358 effect at the high N addition treatment because there was usually less N deposition in the real world than
359 in most field experiments (Adams et al., 2021).

360 Similarly, the senescence rates from leaf and root, the decomposition rates of standing litter, surface
361 litter, fast SOM, slow SOM and passive SOM were regulated by their counterpart C:N ratios (Niu et al.,
362 2010), and this regulation was also reflected in this model (Wang et al., 2022). The N limitation on their
363 senescence rates and decomposition rates were reflected in smaller values in the C-only model than that
364 in the coupled C-N model. Different from LPE, N limitation degree in those variables between the
365 coupled C-N model and the C-only model got similar at the middle N addition rates (N2, N4, N8).
366 Because low-level N additions could alleviate N limitation but high-level N addition would harm plants
367 due to the ionic toxicity (Aber et al., 1998; LeBauer and Treseder, 2008; Niu et al., 2016). That was why
368 the differences in some parameters estimated by the coupled C-N model and the C-only model even got
369 larger at high N addition treatments. However, some other parameters estimated by different models had
370 no significant difference in different N addition treatments. This may be due to the fact that these
371 parameters contain little N limitation information, and therefore these C cycle related processes are not



372 regulated by N processes and can be considered to be resolved processes in both the C-only and coupled
373 C-N models.

374 **4.3 Retrieve nitrogen limitation information from different ecosystem C pools**

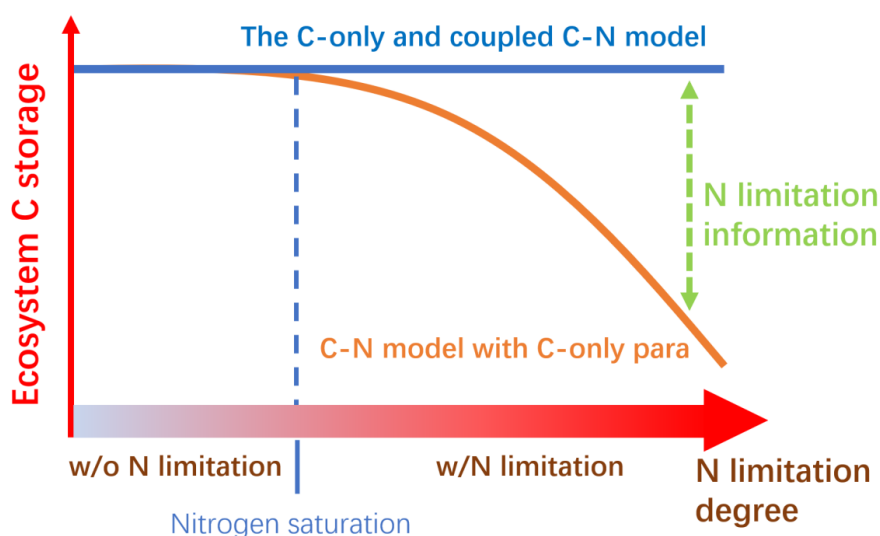
375 Although the N limitation information behind many estimated parameters was different, two models
376 simulated similar pool sizes when two sets of parameters were used in accordance with their different
377 structures (Figure 5). This was reasonable as models with different structures were supposed to similarly
378 simulate the dynamics of the same ecosystem under the same conditions (at every N addition treatment).
379 When we incorporated an N module into the C model, N processes are explicitly simulated, estimated
380 C-related parameters no longer contain N processes for the coupled C-N model, and the N limitation
381 information was retrieved from the C-only model as well.

382 By using the coupled C-N model with parameters estimated by the C-only model to simulate the
383 terrestrial ecosystem C dynamic, the N limitation information behind parameters can be intuitively
384 expressed. Our results showed that GPP, ecosystem C storage in plant and soil pools simulated by the
385 coupled C-N model with the parameters estimated by the C-only model all decreased at the N0 treatment
386 (Figures 5 and 6), but these C pools and GPP change got smaller with the increase of N addition (Figures
387 5 and 6). These results indicated that the parameters estimated in the C-only model did contain the N
388 limitation information, and the limitation degree reduced with increasing N addition rates. If there was
389 no N limitation in observations, the parameters estimated by either the C-only model or coupled C-N
390 model would not contain any N limitation information. Therefore, the C dynamic simulated by the
391 coupled C-N model with the parameters estimated by the C-only model would be consistent to the result
392 simulated by the C-only model. If there was N limitation in observations, the parameters estimated by
393 the C-only model would contain the N limitation information but the parameters estimated by the coupled
394 C-N model would not. Our results that the C fluxes and pools simulated by the coupled C-N model with
395 the parameters estimated by the C-only model was smaller than that simulated by the C-only model,
396 indicate clear N limitation information. The stronger the N limitation, the greater the decrease of the
397 simulation by the coupled C-N model with the parameters estimated by the C-only model (Figures 5 and
398 6).

399 Given that parameter values in their original C-only models were kept or manually tuned for the
400 new models with N processes (Koven et al., 2013; Sokolov et al., 2008; Zaehle and Friend, 2010),



401 predictions by the newly modified ESMs with the N modules mostly predict lower photosynthesis rates,
402 lower C sequestration, and lower ecosystem C storage than their C-only counterpart models. Our results
403 in this study reveal that such predictions of lower C storage with the coupled C-N models than their
404 original models may not reflect reality (Figure 8). In contrast, ESMs may underestimate both future
405 terrestrial C sequestration and the potential C-climate feedback because they overestimate N constraints.



406
407 **Figure 8** The influence of different N limitation degree on the parameterization of the C-only model and the
408 coupled C-N model. Blue line is the C storage simulated by the C-only model or coupled C-N model with data
409 assimilation, orange line is the C storage simulated by the coupled C-N model with parameters estimated by
410 the C-only model.

411 5. Conclusion

412 Based on a 7-year field N addition experiment and data assimilation method, this study carried out an
413 inverse analysis with the C-only model and the coupled C-N model. We found that data assimilation
414 technique could be used to retrieve N limitation information from observations. N limitation information
415 of some C cycle processes can be retrieved by comparing the differences between the parameters
416 estimated by the C-only model and the coupled C-N model with the same observation. N limitation
417 information of the C pools and fluxes can be retrieved by comparing the differences between the C pool
418 dynamic simulated by the coupled C-N model with C-only parameters and the C pool dynamic simulated
419 by the coupled C-N model with its counterpart parameters. In addition, N additions had a unimodal
420 response on most ecosystem component C storage which was mainly determined by their exit rates in



421 this study. In general, we put forward a new method to retrieve N limitation information from
422 observations by data assimilation technique. With the increase of global data products, our method will
423 make it possible to estimate ecosystem nutrient limitation with high reliability and thus provide guidance
424 for policy making or ecosystem management.

425

426 **Data availability**

427 All additional data produced in this study will be published FigShare (10.6084/m9.figshare.22094111)

428

429 **Author contribution:** SW, JW and SN designed the experiments, evaluated the data and wrote the
430 manuscript. CS, YL were involved in the writing (review and editing) of the paper before submissions.

431 WC collected and arranged data. YZ, AY developed the conceptualization and methodology of this study.

432

433 **Competing interests:** The authors declare that they have no conflict of interests.

434 **Acknowledgments**

435 This study was supported by National Key R & D Program of China (2022YFF0802102) and National

436 Science Foundation of China (31988102)

437

438 **Reference**

439 Aber, J., W. McDowell, K. Nadelhoffer, A. Magill, G. Berntson, M. Kamakea, et al. 1998. Nitrogen
440 saturation in temperate forest ecosystems - Hypotheses revisited, *Bioscience*, 48(11), 921-934.

441 Adams, M. A., T. N. Buckley, D. Binkley, M. Neumann, and T. L. Turnbull. 2021. CO₂, nitrogen
442 deposition and a discontinuous climate response drive water use efficiency in global forests,
443 *Nat. Commun.*, 12(1).

444 Bloom, A. A., J.-F. Exbrayat, I. R. Van Der Velde, L. Feng, and M. J. P. o. t. N. A. o. S. Williams. 2016.
445 The decadal state of the terrestrial carbon cycle: Global retrievals of terrestrial carbon allocation,
446 pools, and residence times, 113(5), 1285-1290.

447 Bracken, M. E. S., H. Hillebrand, E. T. Borer, E. W. Seabloom, J. Cebrian, E. E. Cleland, et al. 2015.
448 Signatures of nutrient limitation and co-limitation: responses of autotroph internal nutrient
449 concentrations to nitrogen and phosphorus additions, *Oikos*, 124(2), 113-121.

450 Du, E., C. Terrer, A. F. A. Pellegrini, A. Ahlstrom, C. J. van Lissa, X. Zhao, et al. 2020. Global patterns
451 of terrestrial nitrogen and phosphorus limitation, *Nat Geosci*, 13(3), 221-+.

452 Du, Z., J. Wang, G. Zhou, S. H. Bai, L. Zhou, Y. Fu, et al. 2021. Differential effects of nitrogen vs.
453 phosphorus limitation on terrestrial carbon storage in two subtropical forests: A Bayesian
454 approach, *The Science of the total environment*, 795, 148485-148485.

455 Elser, J. J., M. E. Bracken, E. E. Cleland, D. S. Gruner, W. S. Harpole, H. Hillebrand, et al. 2007. Global
456 analysis of nitrogen and phosphorus limitation of primary producers in freshwater, marine and



- 457 terrestrial ecosystems, *Ecol Lett*, 10(12), 1135-1142.
- 458 Fog, K. J. B. R. 2008. The effect of added nitrogen on the rate of decomposition of organic matter,
459 *Biological Reviews*, 63(3), 433-462.
- 460 Friedlingstein, P., M. O'Sullivan, M. W. Jones, R. M. Andrew, L. Gregor, J. Hauck, et al. 2022. Global
461 carbon budget 2022, 14(11), 4811-4900.
- 462 Hastings, W. K. 1970. Monte-Carlo Sampling Methods Using Markov Chains and Their Applications,
463 *Biometrika*, 57(1), 97-&.
- 464 Hungate, B. A., J. S. Dukes, M. R. Shaw, Y. Q. Luo, and C. B. Field. 2003. Nitrogen and climate change,
465 *Science*, 302(5650), 1512-1513.
- 466 Keeler, B. L., S. E. Hobbie, and L. E. Kellogg. 2009. Effects of Long-Term Nitrogen Addition on
467 Microbial Enzyme Activity in Eight Forested and Grassland Sites: Implications for Litter and
468 Soil Organic Matter Decomposition, *Ecosystems*, 12(1), 1-15.
- 469 LeBauer, D. S., and K. K. Treseder. 2008. Nitrogen limitation of net primary productivity in terrestrial
470 ecosystems is globally distributed, *Ecology*, 89(2), 371-379.
- 471 Leuning, R., F. M. Kelliher, D. G. G. D. Pury, E. D. J. P. C. Schulze, and Environment. 1995. Leaf
472 nitrogen, photosynthesis, conductance and transpiration: scaling from leaves to canopies, *Plant
473 Cell Environment*, 18(10), 1183-1200.
- 474 Liang, J., J. Xia, Z. Shi, L. Jiang, S. Ma, X. Lu, et al. 2018. Biotic responses buffer warming-induced
475 soil organic carbon loss in Arctic tundra, *Glob Chang Biol*, 24(10), 4946-4959.
- 476 Liu, J., X. Li, Q. Ma, X. Zhang, Y. Chen, F. Isbell, et al. 2019. Nitrogen addition reduced ecosystem
477 stability regardless of its impacts on plant diversity, 107(5).
- 478 Luo, Y., and E. A. J. G. C. B. Schuur. 2020. Model parameterization to represent processes at unresolved
479 scales and changing properties of evolving systems, 26(3), 1109-1117.
- 480 Luo, Y., B. Su, W. S. Currie, J. S. Dukes, A. C. Finzi, U. Hartwig, et al. 2004. Progressive nitrogen
481 limitation of ecosystem responses to rising atmospheric carbon dioxide, *Bioscience*, 54(8), 731-
482 739.
- 483 Luo, Y. Q., L. W. White, J. G. Canadell, E. H. DeLucia, D. S. Ellsworth, A. C. Finzi, et al. 2003.
484 Sustainability of terrestrial carbon sequestration: A case study in Duke Forest with inversion
485 approach, *Global Biogeochem Cy*, 17(1).
- 486 Metropolis, N., A. W. Rosenbluth, M. N. Rosenbluth, A. H. Teller, and E. Teller. 1953. Equation of State
487 Calculations by Fast Computing Machines, *J Chem Phys*, 21(6), 1087-1092.
- 488 Niu, S. L., A. T. Classen, J. S. Dukes, P. Kardol, L. L. Liu, Y. Q. Luo, et al. 2016. Global patterns and
489 substrate-based mechanisms of the terrestrial nitrogen cycle, *Ecol Lett*, 19(6), 697-709.
- 490 Niu, S. L., R. A. Sherry, X. H. Zhou, S. Q. Wan, and Y. Q. Luo. 2010. Nitrogen regulation of the climate-
491 carbon feedback: evidence from a long-term global change experiment, *Ecology*, 91(11), 3261-
492 3273.
- 493 Pregitzer, K. S., A. J. Burton, D. R. Zak, and A. F. J. G. C. B. Talhelm. 2010. Simulated chronic nitrogen
494 deposition increases carbon storage in Northern Temperate forests, 14(1), 142-153.
- 495 Quan, Q., F. Y. Zhang, D. S. Tian, Q. P. Zhou, L. X. Wang, and S. L. Niu. 2018. Transpiration Dominates
496 Ecosystem Water-Use Efficiency in Response to Warming in an Alpine Meadow, *J Geophys
497 Res-Bioge*, 123(2), 453-462.
- 498 Song, B., S. L. Niu, L. H. Li, L. X. Zhang, and G. R. Yu. 2014. Soil carbon fractions in grasslands respond
499 differently to various levels of nitrogen enrichments, *Plant Soil*, 384(1-2), 401-412.
- 500 Sullivan, B. W., S. Alvarez-Clare, S. C. Castle, S. Porder, S. C. Reed, L. Schreeg, et al. 2014. Assessing



- 501 nutrient limitation in complex forested ecosystems: alternatives to large-scale fertilization
502 experiments, *Ecology*, 95(3), 668-681.
- 503 Sun, Z., L. Liu, Y. Ma, G. Yin, C. Zhao, Y. Zhang, et al. 2014. The effect of nitrogen addition on soil
504 respiration from a nitrogen-limited forest soil, *Agr Forest Meteorol*, 197, 103-110.
- 505 Tessier, J. T., and D. J. Raynal. 2003. Use of nitrogen to phosphorus ratios in plant tissue as an indicator
506 of nutrient limitation and nitrogen saturation, *J. Appl. Ecol.*, 40(3), 523-534.
- 507 Vicca, S., B. D. Stocker, S. Reed, W. R. Wieder, M. Bahn, P. A. Fay, et al. 2018. Using research networks
508 to create the comprehensive datasets needed to assess nutrient availability as a key determinant
509 of terrestrial carbon cycling, 13(12), 125006.
- 510 Walker, A. P., A. P. Beckerman, L. Gu, J. Kattge, L. A. J. E. Cernusak, and Evolution. 2015. The
511 relationship of leaf photosynthetic traits – V_{cmax} and J_{max} – to leaf nitrogen, leaf phosphorus,
512 and specific leaf area: a meta-analysis and modeling study, *Ecology*, 4(16), 3218-3235.
- 513 Wang, S., Y. Q. Luo, and S. L. Niu. 2022. Reparameterization Required After Model Structure Changes
514 From Carbon Only to Carbon-Nitrogen Coupling, *J Adv Model Earth Sy*, 14(4), 15.
- 515 Wang, S., Q. Quan, C. Meng, W. Chen, Y. Luo, and S. J. J. o. P. E. Niu. 2021. Experimental warming
516 shifts coupling of carbon and nitrogen cycles in an alpine meadow, *J Plant Ecol*.
- 517 Wang, Y. P., R. J. A. Leuning, and F. Meteorology. 1998. A two-leaf model for canopy conductance,
518 photosynthesis and partitioning of available energy. I. Model description and comparison with
519 a multi-layered model, 91(1-2), 89-111.
- 520 Weng, E., and Y. Luo. 2011. Relative information contributions of model vs. data to short- and long-term
521 forecasts of forest carbon dynamics, *Ecol Appl*, 21(5), 1490-1505.
- 522 Xu, T., L. White, D. Hui, and Y. Luo. 2006. Probabilistic inversion of a terrestrial ecosystem model:
523 Analysis of uncertainty in parameter estimation and model prediction, *Global Biogeochem Cy*,
524 20(2), n/a-n/a.
- 525 Yang, H., P. Ciais, Y. L. Wang, Y. Y. Huang, J. P. Wigneron, A. Bastos, et al. 2021. Variations of carbon
526 allocation and turnover time across tropical forests, *Global Ecol Biogeogr*, 30(6), 1271-1285.
- 527 Zong, N., X. Chai, P. L. Shi, and X. C. Yang. 2018. Effects of Warming and Nitrogen Addition on Plant
528 Photosynthate Partitioning in an Alpine Meadow on the Tibetan Plateau, *J. Plant Growth Regul.*,
529 37(3), 803-812.
- 530